Endotoxin-tolerant Mice Have Mutations in Toll-like Receptor 4 (*Tlr4*)

By Salman T. Qureshi,*‖ Line Larivière,‖ Gary Leveque,‖ Sophie Clermont,‖ Karen J. Moore,¶ Philippe Gros,‡‖ and Danielle Malo*§‖

*From the *Department of Medicine, ‡Department of Biochemistry, and §Department of Human Genetics, McGill University, Montreal, Quebec, Canada H3G 1A4; the ‖Centre for the Study of Host Resistance, Montreal General Hospital, Montreal, Quebec, Canada H3G 1A4; and ¶Millennium Pharmaceuticals, Inc., Cambridge, Massachusetts 02139*

Summary

Bacterial lipopolysaccharide (LPS) provokes a vigorous, generalized proinflammatory state in the infected host. Genetic regulation of this response has been localized to the *Lps* locus on mouse chromosome 4, through study of the C3H/HeJ and C57BL/10ScCr inbred strains. Both C3H/HeJ and C57BL/10ScCr mice are homozygous for a mutant *Lps* allele ($Lps^{d/d}$) that confers hyporesponsiveness to LPS challenge, and therefore exhibit natural tolerance to its lethal effects. Genetic and physical mapping of 1,345 backcross progeny segregating this mutant phenotype confined *Lps* to a 0.9-cM interval spanning 1.7 Mb. Three transcription units were identified within the candidate interval, including Toll-like receptor 4 (*Tlr4*), part of a protein family with members that have been implicated in LPS-induced cell signaling. C3H/HeJ mice have a point mutation within the coding region of the *Tlr4* gene, resulting in a nonconservative substitution of a highly conserved proline by histidine at codon 712, whereas C57BL/10ScCr mice exhibit a deletion of *Tlr4*. Identification of distinct mutations involving the same gene at the *Lps* locus in two different hyporesponsive inbred mouse strains strongly supports the hypothesis that altered *Tlr4* function is responsible for endotoxin tolerance.

Key words: lipopolysaccharide • inflammation • positional cloning • *Salmonella* • mice/inbred C3H

Serious infection caused by Gram-negative bacteria is a problem of increasing magnitude, especially among the elderly and immunocompromised populations (1). Virulence and pathogenic potential among this group of organisms are attributed mainly to the presence of LPS, an abundant glycolipid in the outer bacterial membrane (2). The proinflammatory and immunostimulatory properties of LPS are due to the inner conserved lipid A component of LPS; purified lipid A administered in vivo is capable of eliciting a generalized inflammatory response now described as the systemic inflammatory response syndrome (3, 4). To defend against serious infection by Gram-negative bacteria, eukaryotes have developed innate and exquisitely sensitive immunologic surveillance mechanisms that can detect minute quantities of bacterial LPS in vivo. Recognition of LPS by various cell types, including lymphocytes and macrophages, leads to pleiotropic cellular activation and enhanced microbicidal capacities, all of which are aimed at elimination of the inciting pathogen.

Mouse models have been used to characterize the host response to purified LPS for approximately 50 years. Most inbred strains of laboratory mice exhibit reproducible susceptibility to the proinflammatory and toxic properties of LPS. Remarkably, the C3H/HeJ strain exhibits natural tolerance to otherwise lethal doses of LPS, as well as an altered inflammatory response to experimental challenge (5–7). Several cell types derived from the C3H/HeJ strain are hyporesponsive to LPS in vitro. Macrophages fail to develop an activation phenotype or die when exposed to high concentrations of LPS; B lymphocytes do not respond to the mitogenic, adjuvant, or immunogenic properties of LPS, and fibroblasts fail to undergo metabolic activation upon LPS exposure. One consequence of altered endotoxin responsiveness is that C3H/HeJ mice are extremely susceptible to overwhelming infection with virulent Gram-negative bacteria, including *Salmonella typhimurium*, a natural pathogen of both mice and humans (8).

C3H/HeJ mice, along with the C3H/HeN substrain, were both derived from the progenitor strain, C3H/He, in 1947. Neither C3H/He nor C3H/HeN mice have the LPS tolerance phenotype characteristic of C3H/HeJ. Study of LPS responsiveness among several sublines derived from

C3H/HeJ led to the conclusion that the mutant phenotype arose through spontaneous mutation between 1960 and 1968 (9). Initial genetic analysis established that this phenotype is under the control of a single locus, named *Lps*, existing in two allelic forms, Lps^n (responsive) and Lps^d (hyporesponsive) (10). Using the BXH recombinant inbred strain panel, the *Lps* locus was assigned to chromosome 4 by its linkage to *Mup1* (11) and is distinct from the IFN-α gene cluster (*Ifa* [12]). Further genetic mapping using two backcross panels positioned *Lps* between *Mup1* and *Ps* with the following order and map distance: *Mup1*-(6±2)-*Lps*-(13±7)-*Ps* (13). A congenic BALB/c mouse strain containing a 5.5-cM segment of chromosome 4 surrounding the mutant *Lps* locus has been developed and exhibits LPS hyporesponsiveness in vitro and in vivo (14).

Tolerance to the stimulatory properties of LPS has also been observed in the C57BL/10ScCr inbred strain (15). As with C3H/HeJ, the mechanism responsible for LPS tolerance among C57BL/10ScCr mice is unknown. The C57BL/10Sn progenitor strain from which C57BL/10ScCr was derived is LPS responsive, indicating that this mutant phenotype was acquired after 1953. Complementation was not observed among F1 hybrid mice derived from C3H/HeJ and C57BL/10ScCr parents, indicating that both strains have a mutant allele at the *Lps* locus (15).

To identify the nature of LPS hyporesponsiveness in C3H/HeJ mice by positional cloning, we previously localized *Lps* to a 1.1-cM interval through high-resolution genetic mapping of mid-chromosome 4 (16). Through additional genetic mapping, the candidate interval for *Lps* has been narrowed to 0.9 cM between two microsatellite markers, *D4Nds9* and *D4Mit178*, and we have assembled a 1.7-Mb DNA contig spanning this interval. Four unique transcription units were identified within the cloned region, including the gene encoding Toll-like receptor 4 (*Tlr4*)[1] (17). *Tlr4* is an exceptionally strong candidate for the *Lps* mutation based on its chromosomal location, the presence of two independent mutant alleles, and the demonstrated role of members of the TLR family in innate immune recognition of infectious pathogens (18, 19).

Materials and Methods

Fine Genetic Mapping. Procedures for construction of a high-resolution genetic map at the *Lps* locus have been published (16). Using publicly available genetic mapping databases (http://www.informatics.jax.org/maptools.html), one additional informative microsatellite (*D4Nds9*) derived from a flow-sorted 4:6 Robertsonian chromosome library was identified and typed by PCR using flanking oligonucleotides, as described previously (20). An anonymous microdissected clone from the same flow-sorted library (*D4Rck137*; gift of Dr. Jeffrey Friedman, Rockefeller University, New York) was typed by RFLP using TaqI, as described (21).

Identification of Novel Simple Sequence Length Repeats. DNA samples (5 μg) from 10 BAC, 2 P1, and 58 cosmid clones derived from YAC 89A3 were digested with AluI or a combination of HaeIII, AvaII, and HincII using conditions provided by the supplier (New England Biolabs). Individual DNA digests were purified using standard protocols (22), ligated into EcoRV site of pBluescript II KS+ (Stratagene), and transformed to *Escherichia coli* strain XL1-MRF′. Nylon filter replicates (Hybond N; Amersham Life Science) were hybridized in Church's solution at 60°C and probed with poly dAdC:dTdG (Pharmacia Biotech) labeled to high specific activity with [α-^{32}P]dATP by the random-primer method (23). Filters were washed for 30 min at 65°C in 0.5× SSC and 0.1% SDS and exposed for 4–16 h at −70°C using Kodak XAR film and an intensification screen. Plasmid DNA inserts from positive colonies were sequenced by the dideoxy chain termination method (Pharmacia Biotech) to derive flanking primer sequences for *D4Mcg5* to *D4Mcg60*. Oligonucleotide primer pairs for simple sequence length repeat (SSLP) markers *D4Mcg61–D4Mcg86* were identified directly from the sequence of randomly cloned sheared BAC DNA.

Genomic Library Screening and Contig Assembly. Mouse genomic clones corresponding to microsatellites (*D4Nds9*, *D4Mit25*, *D4Mit178*) and the microdissected probe *D4Rck137* were identified from a YAC library (24; Research Genetics) by PCR screening of DNA pools. The primer pair for *D4Rck137* was derived from its nucleotide sequence and amplified a unique 122-bp fragment of the original probe. Genomic clones from a mouse BAC library (25; Research Genetics) were identified by PCR using microsatellites *D4Nds9*, *D4Mit25*, and *D4Mcg6*. P1 clones corresponding to *D4Rck137* and *D4Mit178* were obtained from Genome Systems. Conditions for PCR were essentially as described for genetic mapping except that 1–3 μl of each DNA pool was used as a template. Products were separated on a 7% polyacrylamide gel containing 7 M urea and exposed for 1–7 d at room temperature using Kodak BioMax film. Nucleotide sequencing of the ends of BAC clone inserts was performed using the Thermosequenase radiolabeled terminator cycle sequencing kit (Amersham Life Science). YAC ends were cloned using bubble or inverse PCR methods (26). Additional BAC clones were identified through library screening with oligonucleotide primer pairs derived from nonrepetitive insert-end sequences and SSLPs obtained from BAC and cosmid clones. Assembly of the YAC and BAC/P1 contig spanning the *D4Nds9–D4Mit178* interval was done by sequence-tagged site (STS) content and restriction mapping using rare-cutter enzymes and pulsed field gel electrophoresis (PFGE), as described previously (27).

PFGE Analysis. Genomic DNA from yeast clones containing YACs was prepared in agarose blocks for PFGE analysis (28). Agarose block slices (20 μl) were run undigested or after digestion with NotI, MluI, BssHII, or SacII restriction enzymes (New England Biolabs) using conditions suggested by the supplier. DNA was separated by electrophoresis in a 1% agarose gel (SeaKem GTG; FMC Bioproducts) containing 0.5× TBE (Tris-boric acid-EDTA) using a contour-clamped homogenous electrophoretic field (CHEF DRII; BioRad). Electrophoresis was performed at 130 V for 24 h at 14°C with 15–60-s pulse times to resolve fragments of 50–2,000 kb. DNA of Lambda concatemers and of *Saccharomyces cerevisiae* chromosomes were used as size standards. Southern blots of these gels were prepared, and hybrid-

[1]*Abbreviations used in this paper:* EST, expressed sequence tag; LRR, leucine-rich repeat; NF, nuclear factor; ORF, open reading frame; *PAPPA*, pregnancy-associated plasma protein A; PFGE, pulsed field gel electrophoresis; RACE, rapid amplification of cDNA ends; RT, reverse transcription; SSCP, single-strand conformational polymorphism; SSLP, simple sequence length repeat; STS, sequence-tagged site; TIR, Toll IL-1 receptor; TLR, Toll-like receptor; *Tlr4*, murine Toll-like receptor 4; UTR, untranslated region.

ization was performed using [α-^{32}P]dATP-radiolabeled single-copy probes from the region, total mouse genomic DNA, and pBR322 sequences specific for each arm of the pYAC4 vector.

Subcloning of DNA Inserts from YAC Clones. Agar-embedded genomic DNA from individual yeast clones carrying YAC 89A3 was partially digested with Sau3AI to produce an average fragment size of 30–50 kb and ligated into the BamHI cloning site of the cosmid vector, SuperCosI (Stratagene). The ligation mixture was packaged in vitro (Gigapack II Gold; Stratagene) and used to infect *E. coli* XL1-MRF′, which was subsequently plated on LB agar containing 100 μg/ml ampicillin. Replicate filters (Hybond N; Amersham Life Science) were made for each plate and hybridized with [α-^{32}P]dATP-radiolabeled total mouse genomic DNA to identify cosmids containing mouse inserts. Positive colonies were selected and expanded in culture, and cosmid DNA was purified by standard protocols (22). 71 cosmid subclones were ordered relative to the originating YAC 89A3 and the BAC contig by restriction mapping with EcoRI, and by hybridization of total genomic DNA as described previously (29) and specific probes derived from the *Lps* candidate region.

cDNA Selection. Direct cDNA selection was performed on BAC clones or cosmids according to the method of Rommens et al. (30). 6–10 μg of BAC or cosmid DNA was electrophoresed in 0.9% agarose gel (SeaKem GTG) and immobilized on a nylon membrane (Hybond N) by Southern transfer. Two rounds of hybridization were conducted in Church's solution at 60°C for 72 h using 1 μg each of mouse cDNA prepared from mouse spleen, hypothalamus, heart, kidney, testis, and skin polyA$^+$ RNA. Selected cDNA was PCR-amplified with the oligonucleotide $(CUA)_4$GCGGAATTCTCGAGATCT and cloned by using the uracil DNA glycosylase cloning system (GIBCO BRL). Automated sequencing of cDNA was performed using an ABI 373 apparatus (Applied Biosystems). Sequences were compared with nucleotide, expressed sequence tag (EST), and protein databases using the BLAST server (http://www.ncbi.nih.nlm.gov/cgi-bin/BLAST/); repetitive elements were identified using RepeatMasker.

Sheared BAC Library Construction. Individual BAC clones comprising the minimal tiling path across the *Lps* region were cultured overnight in 500–1,000 ml of LB broth with 12.5 μg/ml chloramphenicol, and plasmid DNA was purified using Midi or Maxi Prep kits (QIAGEN). Random shearing was performed by passing argon through an AeroMist nebulization chamber (CisUs, Inc.) containing 50–100 μg BAC DNA in 1.5 ml of shearing buffer (35 mM Tris-HCl, pH 8.0, 15 mM $MgCl_2$, 25% glycerol) for 5–15 min. DNA ends were repaired with T4 polynucleotide kinase and T7 DNA polymerase using conditions recommended by the supplier (New England Biolabs). Samples were electrophoresed in 1.5% low-melting-point agarose gel in 1× TAE (Tris-acetic acid-EDTA), and fragments of 1.5–3.0 kb in size were excised and purified using β-agarase. Ligation of phosphorylated linkers (oligo 1, 5′-CTCTAAAG-3′, and oligo 2, 5′-CTTTAGAGCACA-3′, were mixed in a 1:1 ratio and annealed by heating to 95°C for 10 min followed by cooling to room temperature) in 100-fold molar excess was done overnight at 16°C. Linkers were removed by centrifugation for 5 min at 6,000 rpm through a 40-bp MWCO column (Millipore) followed by electrophoresis in 1.5% low-melting-point agarose. Linkered DNA was purified with β-agarase, ligated into the BstxI site of pmin, and transformed to DH10β competent cells (GIBCO BRL). Automated sequencing of 960 subclones was performed for each sheared BAC; nucleotide sequences were compared with nucleotide, protein, and EST databases using BLAST.

Northern and Southern Blotting. Mouse multiple tissue polyA$^+$ Northern blots (Clontech) were hybridized with [α-^{32}P]dATP-radiolabeled probes obtained by direct selection (*1d8*), cDNA library screening (*3f3*), or reverse transcription (RT)-PCR (*Tlr4*). Hybridization was done at 42°C in a mixture of 50% formamide, 5× SSC, 1% SDS, 10% dextran sulfate, 1× Denhardt's solution, 0.02 M Tris (pH 7.5), and denatured herring sperm DNA (200 μg/ml) for 16 h with final washing at 65°C for 30 min in 0.2× SSC, 0.1% SDS. Autoradiography was performed with Kodak XAR film at −70°C and an intensifying screen for 16 h. Southern blots of genomic DNA (5 μg) from C57BL/6J, C3H/HeJ, DBA/2J, and C57BL/10ScCr mouse strains that had been digested with either HindIII or BamHI as described (16) were probed with [α-^{32}P]dATP radiolabeled 0.65-, 1.2-, and 2.9-kb probes corresponding to nucleotides 1–649, 243–1443, and 1–2943 of the *Tlr4* coding sequence using the same conditions as for Northern blots; the final wash was performed with 0.5× SSC and 0.1% SDS.

cDNA Library Screening. Approximately 10^6 clones of a λgt11 pre-B cell line 70/Z3 cDNA library were plated and screened with the *3f3* probe isolated by cDNA selection following standard techniques (22). Positive phages were plaque purified, and phage DNA was isolated according to standard procedures. The inserts of positive clones were released by EcoRI digestion, subcloned into the EcoRI site of pBluescript II (KS+) vector (Stratagene), and PCR cycle-sequenced (Amersham Life Science). Overlapping sequences were aligned to obtain the complete open reading frame (ORF) of *3f3*.

RT-PCR. Total spleen RNA from C57BL/6J, C3H/HeJ, and C57BL/10ScCr mouse strains was extracted using Trizol (GIBCO BRL) and used to isolate strain-specific cDNA clones for *Tlr4*. First-strand cDNA synthesis was carried out using 2 μg of total RNA, 100 ng of random hexamers, and 200 U of Moloney murine leukemia virus reverse transcriptase (GIBCO BRL). The reaction conditions for cDNA synthesis were as described previously (29). *Tlr4* cDNA clones were obtained by PCR amplification of three overlapping fragments covering the entire coding region of the mRNA. Fragment A was 710 bp in length and was amplified using primers 5′-TCTGCCCTGCCACCATTTAC-3′ and 5′-ACATGTCTAAAGAGAGATTGAC-3′; fragment B was 1,190 bp in length and was amplified using primers 5′-GCTGGATTTATCCAGGTG-3′ and 5′-GAAAGAATTGCCAGCCATTTT-3′; and fragment C was 1,681 bp in length and was amplified using primers 5′-AGCTGCAGCACCTGGATTT-3′ and 5′-AAATTGGAATGAAGACCTCTCA-3′. Amplified products were directly sequenced using the Thermosequenase radiolabeled terminator cycle sequencing kit.

Single-strand Conformational Polymorphism Analysis. To detect single nucleotide changes in alleles of different inbred mouse strains, radiolabeled PCR products were denatured and electrophoresed on 6% polyacrylamide gels containing 5% glycerol at 30 W for 4–6 h at room temperature. The nucleotide sequences of polymorphisms detected by single-strand conformational polymorphism (SSCP) analysis were determined with the Thermosequenase radiolabeled terminator cycle sequencing kit.

Identification of ESTs Mapping to the Lps Interval. 40 ESTs from the Human Transcript Map (http://www4.ncbi.nih.nlm.gov/science96/) corresponding to map positions *D9S160* and *D9S258* were obtained from the IMAGE consortium (31) via Research Genetics. Clone inserts were isolated according to the suppliers' protocols and individually hybridized to dot blots of BAC DNA from the *Lps* candidate region after [α-^{32}P]dATP radiolabeling. Hybridization was performed for 16 h at 55°C in 6×

SSC, 5× Denhardt's solution, 0.5% SDS, and denatured herring sperm DNA (200 μg/ml); final washing was performed at 55°C for 15–30 min in 0.5× SSC, 0.1% SDS. Autoradiography was performed using Kodak XAR film with an intensifying screen for 4–16 h at −70°C.

Rapid Amplification of cDNA Ends. 5′- and 3′-rapid amplification of cDNA ends (RACE) were performed with Marathon-ready mouse spleen cDNA (0.5 ng) using the Advantage cDNA PCR kit (Clontech). Various gene-specific primers derived from our *Tlr4* sequence were used in conjunction with the AP1 and AP2 primers to perform primary and secondary nested PCR. After electrophoresis in 1.5% low-melting-point agarose gel, amplification products were excised and purified using β-agarase (New England Biolabs). Cycle sequencing was performed with gene-specific primers using the Thermosequenase radiolabeled terminator cycle sequencing kit (Amersham Life Science).

Results

Lps Maps to a 0.9-cM Interval Spanning 1.7 Mb. Previously, we reported the construction of a high-resolution linkage map encompassing the *Lps* locus, using 597 (DBA/2J × C3H/HeJ)F1 × C3H/HeJ and 748 (C57BL/6J × C3H/HeJ)F1 C3H/HeJ backcross progeny segregating the recessive mutant ($Lps^{d/d}$) phenotype and a preexisting interspecific backcross panel of 259 (*Mus spretus* × C57BL/6J)F1 × C57BL/6J (13). LPS hyporesponsiveness, identified by an absent splenocyte mitogenic response after in vitro stimulation, as well as susceptibility to in vivo infection with *S. typhimurium*, was compared with allelic inheritance of SSLP markers originating from mid-chromosome 4. Both phenotypes were concordantly inherited and localized within a 1.1-cM interval to which no candidate genes had previously been mapped. To refine the location of *Lps*, additional SSLPs obtained from public databases (http://www.informatics.jax.org/) as well as 7 informative microsatellites among 86 novel (*D4Mcg*) markers derived from our cloned DNA contig were mapped in recombinant progeny (Table I). *D4Mcg* markers were isolated either by [CA]n screening of small-insert libraries constructed from P1 clones (5226, 5227), BAC clones (243o20, 358p4, 302p22), and 58 cosmids derived from YAC 89A3, or via sequence analysis of clones obtained by cDNA selection and randomly cloned sheared BAC libraries. Five of these SSLPs did not recombine with *Lps* among 748 (*D4Mcg6*, *D4Mcg21*) or 1,345 (*D4Mcg24*, *D4Mcg25*, *D4Mcg27*) meioses tested. *D4Mcg10* mapped 0.3 cM centromeric to *D4Nds9*, and *D4Mcg5* cosegregated with the distal flanking marker *D4Mit178*, confining the genetic interval containing *Lps* to 0.9 cM (Fig. 1 A). Most of the other novel *D4Mcg* markers were informative in the interspecific backcross panel (data not shown) and useful in assembly of the DNA contig spanning this interval.

A 1.7-Mb genomic DNA contig encompassing the *Lps* locus was constructed using flanking (*D4Nds9*, *D4Mit178*) and internal (*D4Mit25*, *D4Rck137*) markers as entry probes for a bidirectional chromosome walk within YAC, BAC, and P1 libraries. A total of 31 YAC, 29 BAC, and 5 P1 clones that together form a robust contig across the candidate interval for *Lps* were sequentially identified through repeated isolation of novel internal or end-insert markers from previously identified clones, followed by rescreening of 1 or more libraries. All clones were ordered by se-

Table I. *New Polymorphic Markers Mapped to the Lps Region*

Locus	Probe	Repeat unit*	Primers 5′ → 3′	Allele size	Polymorphism‡
				bp	
P1-5227	*D4Mcg5*	$[CT]_{23}\,[GT]_{23}$	F: GGGAGGATGTAAAGCTTGAT	141	H>B=D>S
			R: CCAACATCCTCTTACCTCCA		
P1-5226	*D4Mcg6*	$[GT]_{24}$	F: GCATAGGAACAGCTTCTGTGT	122	H=D>B
			R: TTCTATAAATAAGTACCT		
Bac243o20	*D4Mcg10*	$[CA]_4TA[CA]_{25}$	F: TCCTCAGTCACACTAGATTG	120	B=D>H>S
			R: TAGCCTGTGGTGTGATTAGTT		
Yac89a3	*D4Mcg21*	$[GT]_{19}N_{22}[AT]_{11}$	F: CAGGGAGGCATATTCATA	168	H=D<B<S
			R: TCTAATTGCCTTTCAATC		
Yac89a3	*D4Mcg24*	$[GT]_{16}$	F: GGTACCTCTATTAGGTGAATC	113	S>H>B=D
			R: ACAGTCTGACCTAGGTAGAGG		
Yac89a3	*D4Mcg25*	$[CA]_{24}$	F: CCATGCTGGGAATCTCACAAC	164	D<H=B<S
			R: CTATTCTAGAGCCAGTCATTTC		
Yac89a3	*D4Mcg27*	$[GT]_{25}$	F: CTTTCATTAGACAGATTATAT	140	H>B=D>S
			R: CAGACAGTATGAACTCCTG		

*The base composition of each simple sequence repeat is indicated. A, adenine; C, cytosine; G, guanine; T, thymidine. Numeric subscripts denote the length of each dinucleotide repeat shown in brackets. N_{22} = 22-bp nonrepetitive sequence.
‡Relative allele sizes among inbred mouse strains as generated by PCR using flanking forward (F) and reverse (R) primers. B, C57BL/6J; D, DBA/2J; H, C3H/HeJ; S, *M. spretus*.

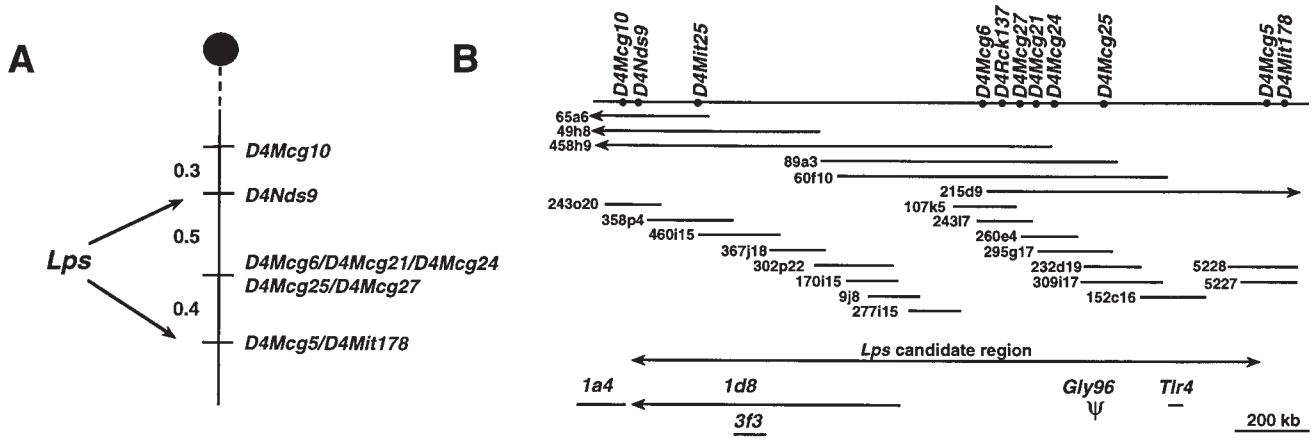

Figure 1. Schematic representation of the *Lps* candidate region. (A) Genetic map of the *Lps* interval. A genetic map of mouse chromosome 4 was generated from haplotype analysis of 1,345 backcross progeny segregating the *Lps* phenotype. The *Lps* locus was mapped between *D4Nds9* and *D4Mit178*. Genetic distances are given to the left in cM. (B) Physical map of the *Lps* region. Solid bar, genomic DNA. The order of markers was established based on the YAC, BAC, and P1 contig. Unique clone addresses are indicated. Arrow, the candidate *Lps* region. There are six unresolved recombination events between the proximal marker *D4Nds9* and *D4Mcg6*, and five unmapped crossovers between *D4Mcg25* and *D4Mcg5*. The position of the four transcription units and the pseudogene identified within the candidate region is shown immediately below the cloned contig. The direction of the transcription is shown for clone *1d8*.

quence-tagged site (STS) content mapping and sized by PFGE; only those used for generation of novel probes or transcription unit identification are shown (Fig. 1 B). The integrity of clones was confirmed by mapping of informative novel probes in the interspecific backcross panel and/or by Southern hybridization to DNA derived from the contig.

Tlr4 and Two Novel Genes Map within the Lps Candidate Region. Direct cDNA selection, sequence analysis of randomly cloned sheared BAC DNA from our contig, and comparative mapping of ESTs and genes that had been assigned to regions of human chromosome 9 syntenic with mouse chromosome 4 were used for transcript identification. Three transcription units corresponding to the DNA contig spanning the *Lps* locus were initially identified by direct cDNA selection. Two rounds of hybridization with expanded cDNA from heart, hypothalamus, skin, testis, kidney, and spleen were performed on 13 BAC clones and 5 cosmid clones, yielding a total of 516 selected cDNA. 95 repeat-free mouse DNA fragments were identified by partial sequence analysis; 35 of these specifically hybridized to clones of the DNA contig at 12 distinct positions. Unique transcription units corresponding to three cDNA clones (*1a4*, *1d8*, *3f3*) were identified through a combination of Northern blot analysis and database comparisons (Fig. 2). Clone *1a4* exhibited significant sequence homology to human pregnancy-associated plasma protein A (*PAPPA*; reference 32), and mapped to BAC 243o20, the most proximal clone in the contig. Human *PAPPA* had previously been mapped to chromosome 9q33.1, a region known to be homologous to a portion of mouse chromosome 4 proximal to *Lps*. Northern blot analysis with clone *3f3* revealed a single ~3.7-kb transcript that was most highly expressed in the mouse brain, and visible in all other tissues. Using *3f3* to probe a pre-B cell cDNA library, a set of overlapping clones mapping specifically to BAC 460i15 was isolated. Sequence analysis revealed that the transcription unit corresponding to *3f3* has an ORF of 1,959 bp encoding 653 amino acids. At the nucleotide level, this transcript is 85% homologous to a human zinc finger protein (sequence data available from EMBL/GenBank/DDBJ under accession no. U18543) known to interact with the activation domain of lentiviral Tat proteins (33). Northern blot analysis with

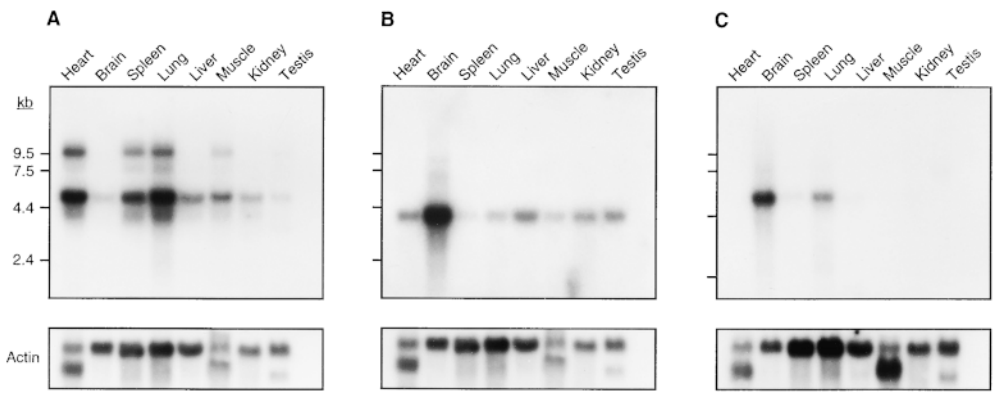

Figure 2. Expression analysis of three transcription units identified within the *Lps* candidate region. Mouse multiple-tissue Northern blots of polyA$^+$ RNA (Clontech) were hybridized with (A) *Tlr4*; (B) clone *3f3*; and (C) clone *1d8*. β-actin was used as control. Exposure times were all 24 h and reflect the relative abundance of each transcript. RNA size markers (in kb) are shown on the left side of each autoradiogram.

1d8 revealed a single ~6-kb transcript most strongly expressed in the brain, with lower expression levels in the lung, spleen, and liver, and no detectable message in other tissues. This clone shares 68% nucleotide homology to mouse astrotactin (EMBL/GenBank/DDBJ accession no. U48797), a ligand for neuron-glia binding during neuronal migration (34). Southern hybridization of additional probes (human EST WI-14828 corresponding to human IMAGE clone 46391 [31] and mouse partial cDNA clones) corresponding to different regions of the same transcription unit demonstrated that the genomic DNA encoding this astrotactin homologue spans ~750 kb of the proximal half of the BAC contig (Fig. 1 B). A fourth transcription unit was identified by comparative mapping. The human Toll-like receptor 4 gene (*TLR4*; sequence data available from EMBL/GenBank/DDBJ under accession no. U93091) maps to chromosome 9q32-33 and is a member of an emerging family of molecules implicated in innate immune recognition (17). PCR primers derived from the human and rat sequences (EMBL/GenBank/DDBJ accession no. AF057025) were used to localize mouse *Tlr4* to BAC 152c16. Northern blot analysis using a 1.2-kb partial mouse *Tlr4* cDNA probe revealed expression of an ~5-kb transcript in all tissues, corresponding to the length of the cDNA we have cloned. An ~9-kb transcript was also detected in heart, spleen, lung, muscle, and testis. The transcription unit corresponding to *Pappa* was excluded as a candidate *Lps* gene because it mapped outside the *Lps* candidate region defined by *D4Nds9* and *D4Mit178*. Although the three genes corresponding to *1d8*, *3f3*, and *Tlr4* are candidate *Lps* genes based on their expression in reticuloendothelial organs and location within the *Lps* candidate region, we chose to focus our analysis on *Tlr4* because of its homology to a gene family including *Drosophila Toll* and *TLR2*, both of which are components of the innate immune response and capable of mediating LPS-induced cell signaling (18, 19).

The Amino Acid Sequence of Human and Mouse Tlr4 Is Highly Conserved. *Tlr4* cDNA fragments were isolated by RT-PCR using primers derived from the human *TLR4* gene (EMBL/GenBank/DDBJ accession no. U93091) and a rat EST (accession no. AF057025) sequence that shows strong homology with the human *TLR4* gene. We determined the sequence of a 3,864 bp cDNA containing one 2,505-bp ORF predicted to encode a protein of 835 amino acids (Fig. 3). Our sequence, combined with estimation of the lengths of the 5′ and 3′ untranslated regions (UTRs) by RACE PCR (data not shown), corresponds to the smaller transcript observed by Northern blot analysis. The nature of the larger mouse transcript identified by our *Tlr4* probe will require further investigation. In humans, two transcripts of ~5.5 and ~4.4 kb are present in all tissues, with predominant expression in the spleen and peripheral blood leukocytes. The observed size difference of the two human *TLR4* transcripts was explained by differential splicing of the 3′ UTR (18).

The predicted amino acid sequence of mouse *Tlr4* was aligned with the corresponding human protein (Fig. 3). The mouse Tlr4 sequence is homologous (67% identical, 79% similar at the amino acid level) over its entire length to human TLR4, a type I transmembrane protein with an extracellular leucine-rich repeat (LRR) domain and a cytoplasmic Toll IL-1 receptor (TIR) homology signaling domain (18). Several imperfect LRRs were identified by sequence and pattern analysis of the extracellular segment of mouse Tlr4 using the program PRINTS (http://www.biochem.ucl.ac.uk/bsm/dbbrowser/PRINTS/PRINTS.html). LRRs are found in a variety of protein families with widely different functions and are thought to be involved in mediating protein–protein interactions (35). Amino acid conservation between the mouse and human TLR4 is stronger in the cytoplasmic signaling domain compared with the extracellular portion of the protein (89 vs. 68%). The intracytoplasmic segment corresponding to TIR signaling domain is a core module shared by TLR genes, IL-1R, mammalian MyD88 factors, and plant disease resistance proteins (36).

```
Mouse:   1   MMPPWLLARTLIMAL-FFSCLTPGSLNPCIEVVPNITYQCMDQKLSKVPDDIPSSTKNID  59
             MM    LA TLI A+ F SC+ P S  PC+EVVPNITYQCM+    K+PD++P STKN+D
Human:   1   MMSASRLAGTLIPAMAFLSCVRPESWEPCVEVVPNITYQCMELNFYKIPDNLPFSTKNLD  60

Mouse:  60   LSFNPLKILKSYSFSNFSELQWLDLSRCEIETIEDKAWHGLHHLSNLILTGNPIQSFSPG 119
             LSFNPL+ L SYSF +F ELQ LDLSRCEI+TIED A+  L HLS LILTGNPIQS + G
Human:  61   LSFNPLRHLGSYSFFSFPELQVLDLSRCEIQTIEDGAYQSLSHLSTLILTGNPIQSLALG 120

Mouse: 120   SFSGLTSLENLVAVETKLASLESFPIGQLITLKKLNVAHNFIHSCKLPAYFSNLTNLVHV 179
             +FSGL+SL+ LVAVET LASLE+FPIG L TLK+LNVAHN I S KLP YFSNLTNL H+
Human: 121   AFSGLSSLQKLVAVETNLASLENFPIGHLKTLKELNVAHNLIQSFKLPEYFSNLTNLEHL 180

Mouse: 180   DLSYNYIQTITVNDLQFLRENPQVNLSLDMSLNPIDFIQYQAFQGIKLHELTLRGNFNSS 239
             DLS N IQ+I   DL+ L + P +NLSLD+SLNP++FIQ  AF+ I+LH+LTLR NF+S
Human: 181   DLSSNKIQSIYCTDLRVLHQMPLLNLSLDLSLNPMNFIQPGAFKEIRLHKLTLRNNFDSL 240

Mouse: 240   NIMKTCLQNLAGLHVHRLILGEFKDERNLEIFEPSIMEGLCDVTIDEFRLTYTNDFSDDI 299
             N+MKTC+Q LAGL VHRL+LGEF+-E NLE F+ S +EGLC++TI+EFRL Y + + DDI
Human: 241   NVMKTCIQGLAGLEVHRLVLGEFRNEGNLEKFDKSALEGLCNLTIEEFRLAYLDYYLDDI 300

Mouse: 300   VK-FHCLANVSAMSLAGVSIKYLEDVPKHFKWQSLSIIRCQLKQFPTLDLPFLKSLTLTM 358
             +  F+CL NVS+ SL  V+I+ ++D   +F WQ L ++ C+  QFPTL L  LK LT T
Human: 301   IDLFNCLTNVSSFSLVSVTIERVKDFSYNFGWQHLELVNCKFGQFPTLKLKSLKRLTFTS 360

Mouse: 359   NKGSISFKKVALPSLSYLDLSRNALSFSGCCSYSDLGTNTLRHLDLSFNGAIIMSANFMG 418
             NKG  +F +V LPSL +LDLSRN LSF GCCS SD GT +L++LDLSFNG I MS+NF+G
Human: 361   NKGGNAFSEVDLPSLEFLDLSRNGLSFKGCCSQSDFGTTSLKYLDLSFNGVITMSSNFLG 420

Mouse: 419   LEELQHLDFQHSTLKRVTEFSAFLSLEKLLYLDISYTNTKIDFDGIFLGLTSLNTLKMAG 478
             LE+L+HLDFQHS LK+++EFS FLSL  L+YLDIS+T+T++ F+GIF GL+SL  LKMAG
Human: 421   LEQLEHLDFQHSNLKQMSEFSVFLSLRNLIYLDISHTHTRVAFNGIFNGLSSLEVLKMAG 480

Mouse: 479   NSFKDNTLSNVFANTTNLTFLDLSKCQLEQISWGVFDTLHRLQLLNMSHNNLLFLDSSHY 538
             NSF++N L ++F    NLTFLDLS+CQLEQ+S   F++L  LQ+LNMSHNN   LD+  Y
Human: 481   NSFQENFLPDIFTELRNLTFLDLSQCQLEQLSPTAFNSLSSLQVLNMSHNNFFSLDTFPY 540

Mouse: 539   NQLYSLSTLDCSFNRIETS-KGILQHFPKSLAFFNLTNNSVACICEHQKFLQWVKEQKQF 597
               L SL  LD S N I TS K  LQHFP SLAF NLT N  AC CEHQ FLQW+K+Q+Q
Human: 541   KCLNSLQVLDYSLNHIMTSKKQELQHFPSSLAFLNLTQNDFACTCEHQSFLQWIKDQRQL 600

Mouse: 598   LVNVEQMTCATPVEMNTSLVLDFNNSTCYMYKTIISVSVVSVIVVSTVAFLIYHFYFHLI 657
             LV VE+M CATP +     VL   N TC M KTII VSV+SV+VVS VA L+Y FYFHL+
Human: 601   LVEVERMECATPSDKQGMPVLSL-NITCQMNKTIICVSVLSVLVVSVVAVLVYKFYFHLM 659

Mouse: 658   LIAGCKKYSRGESIYDAFVIYSSQNEDWVRNELVKNLEEGVPRFHLCLHYRDFIPGVAIA 717
             L+AGC KY RGE+IYDAFVIYSSQ+EDWVRNELVKNLEEGVP F LCLHYRDFIPGVAIA
Human: 660   LLAGCIKYGRGENIYDAFVIYSSQDEDWVRNELVKNLEEGVPPFQLCLHYRDFIPGVAIA 719

Mouse: 718   ANIIQEGFHKSRKVIVVVSRHFIQSRWCIFEYEIAQTWQFLSSRSGIIFIVLEKVEKSLL 777
             ANII EGFHKSRKVIVVVS+HFIQSRWCIFEYEIAQTWQFLSSR+GIIFIVL+KVEK+LL
Human: 720   ANIIHEGFHKSRKVIVVVSQHFIQSRWCIFEYEIAQTWQFLSSRAGIIFIVLQKVEKTLL 779

Mouse: 778   RQQVELYRLLSINTYLEWEDNPLGRHIFWRRLKNALLDGKASNPEQTAEEEQETATWT   835
             RQQVELYRLLS NTYLEWED+ LGRHIFWRRL+ ALLDGK+ NPE T          T
Human: 780   RQQVELYRLLSRNTYLEWEDSVLGRHIFWRRLRKALLDGKSWNPEGTVGTGCNWQEATSI 841
```

Figure 3. Predicted 835 amino acid sequence of the mouse *Tlr4* gene. Amino acid positions are numbered from the start of the 2.5-kb ORF. The protein sequences of mouse Tlr4 (top) and human TLR4 (bottom; EMBL/GenBank /DDBJ accession no. U93091) are aligned. Amino acid identity is shown between the two sequences; a + represents similarity between the corresponding pair of amino acid residues. The predicted transmembrane domain is underlined. The position of the proline to histidine substitution at position 712 associated with LPS hyporesponsiveness is highlighted in bold. These sequence data are available from EMBL/GenBank/DDBJ under accession no. AF110133.

Mouse Tlr4 exhibits a lower degree of homology (40–46% similarity) with other members of the Toll family, including human TLR1, TLR2, TLR3, TLR5, and RP105.

Endotoxin-hyporesponsive Mice Have Unique, Distinct Mutations in Tlr4. Three pairs of oligonucleotide primers were used to analyze mRNA transcripts from C3H/HeJ ($Lps^{d/d}$) and C57BL/6J ($Lps^{n/n}$) mouse strains by RT-PCR for the presence of sequence alterations in the coding portion of the *Tlr4* gene. The only significant mutation detected was a C to A transversion resulting in a single nonconservative amino acid substitution (proline^{712} to histidine^{712}) within the cytoplasmic domain of *Tlr4* of the LPS-tolerant C3H/HeJ strain (Fig. 4 A). To compare the segregation of *Tlr4* with the *Lps* phenotype, PCR primers (5′-GTGCCCCGCTTTCACCTCTG-3′ and 5′-TCTAGACACTACCACAATAA-3′) flanking the region predicted to contain the C3H/HeJ mutation were used to amplify genomic DNA from our two panels of recombinant animals. No recombinants were detected among 1,345 meioses, as the C to A transversion showed perfect cosegregation with the *Lps* phenotype. Since the Pro^{712} to His^{712} missense mutation identified in C3H/HeJ *Tlr4* does not suggest an obvious loss

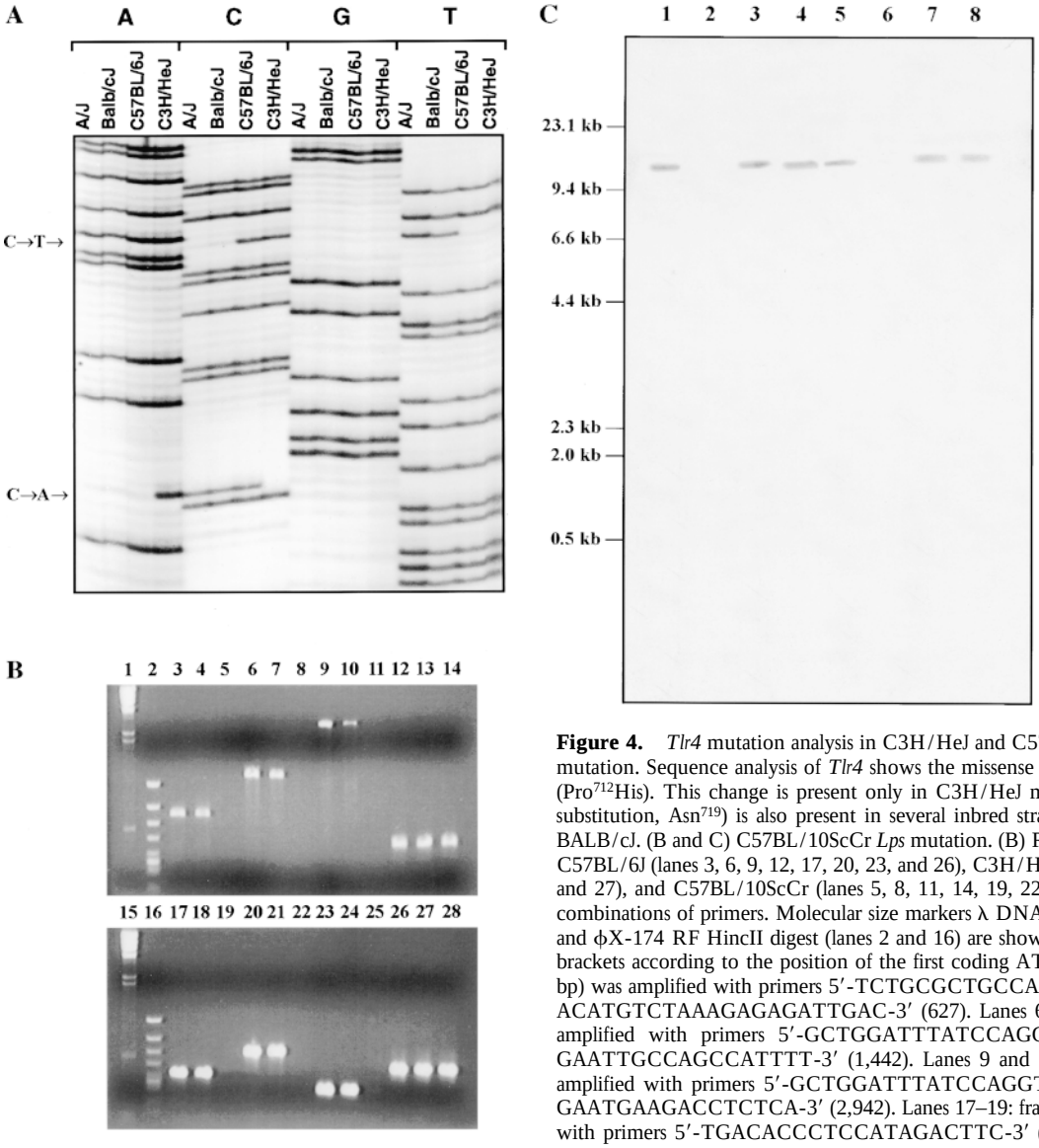

Figure 4. *Tlr4* mutation analysis in C3H/HeJ and C57BL/10ScCr. (A) C3H/HeJ *Lps* mutation. Sequence analysis of *Tlr4* shows the missense mutation, a C to A transversion (Pro^{712}His). This change is present only in C3H/HeJ mice. A silent mutation (C to T substitution, Asn^{719}) is also present in several inbred strains of mice, including A/J and BALB/cJ. (B and C) C57BL/10ScCr *Lps* mutation. (B) RT-PCR of spleen mRNA from C57BL/6J (lanes 3, 6, 9, 12, 17, 20, 23, and 26), C3H/HeJ (lanes 4, 7, 10, 13, 18, 21, 24, and 27), and C57BL/10ScCr (lanes 5, 8, 11, 14, 19, 22, 25, and 28) using six different combinations of primers. Molecular size markers λ DNA-HindIII digest (lanes 1 and 15) and ϕX-174 RF HincII digest (lanes 2 and 16) are shown. Primer positions are given in brackets according to the position of the first coding ATG. Lanes 3–5: fragment A (696 bp) was amplified with primers 5′-TCTGCGCTGCCACCAGTTAC-3′ (−69) and 5′-ACATGTCTAAAGAGAGATTGAC-3′ (627). Lanes 6–8: fragment B (1,200 bp) was amplified with primers 5′-GCTGGATTTATCCAGGTG-3′ (242) and 5′-GAAAGAATTGCCAGCCATTTT-3′ (1,442). Lanes 9 and 10: fragment C (2,700 bp) was amplified with primers 5′-GCTGGATTTATCCAGGTG-3′ (242) and 5′-AAATTGGAATGAAGACCTCTCA-3′ (2,942). Lanes 17–19: fragment D (409 bp) was amplified with primers 5′-TGACACCCTCCATAGACTTC-3′ (1,541) and 5′-GGTATATCAGAAATGCTACA-3′ (1,950). Lanes 20–22: fragment E (641 bp) was amplified with primers 5′-GTCCTTGAGAAGGTTGAGAAGTCCC-3′ (2,301) and 5′-AAATTGGAATGAAGACCTCTCA-3′ (2,942). Lanes 23–25: fragment F (299 bp) was amplified with primers 5′-GAAGGAAGTAGCACTGACACCTTC-3′ (2,643) and 5′-AAATTGGAATGAAGACCTCTCA-3′ (2,942). Lanes 12–14 and 26–28: *Gapdh* (459 bp) was amplified with primers 5′-TTTGTGATGGGTGTGAACCACGAG-3′ and 5′-GGAGACAACCTGGTCCTCAGTGTA-3′. A single *Tlr4* product of the expected size is seen only in RT-PCR of spleen mRNA from C57BL/6J and C3H/HeJ, although *Gapdh* mRNA was amplified from all RT-PCR samples including C57BL/10ScCr. (C) Southern blot analysis of chromosomal rearrangement associated with the C57BL/10ScCr *Lps* allele. Southern blot of a *Tlr4* partial cDNA (position 242–1442) hybridized to C57BL/6J (lanes 1 and 5), C57BL/10ScCr (lanes 2 and 6), C3H/HeJ (lanes 3 and 7), and DBA/2J (lanes 4 and 8) DNA digested with BamHI (1– 4) or HindIII (5–8). Size markers (in kb) are indicated to the left of the autoradiogram.

of function, the corresponding region was PCR-amplified using genomic DNA from 46 classical and wild-derived mouse strains and analyzed for nucleotide changes by SSCP and sequencing. Of three different migration patterns detected by SSCP, one was unique to C3H/HeJ mice, whereas the second and third patterns were present in 12 and 34 mouse strains, respectively (Table II). Sequence analysis confirmed that the unique C3H/HeJ SSCP pattern is caused by the C to A transversion at codon 712 (CCT to CCA, Pro^{712} to His^{712}) and that the two other SSCP patterns resulted from a silent mutation (T to C transition) at codon Asn^{719} (Table II, and Fig. 4 A). *Tlr4* cDNA from the C57BL/10ScCr ($Lps^{d/d}$) mouse strain was not amplified with any of these primer pairs (Fig. 4 B). Therefore, five additional primer pairs covering the entire coding region and the 3′ UTR of the mouse *Tlr4* cDNA were used to amplify RT RNA from the spleens of normal and mutant mice. PCR amplification products of the anticipated size were generated with all sets of primers using RT RNA from normal C57BL/6J and LPS-hyporesponsive C3H/HeJ strains, whereas no PCR products were obtained using C57BL/10ScCr spleen RT RNA (Fig. 4 B). A control *Gapdh* RT-PCR product was generated in all mouse species examined. Southern blot analysis of genomic DNA from normal (C57BL/6J and DBA/2J) and LPS-hyporesponsive (C3H/HeJ and C57BL/10ScCr) mice revealed the absence of hybridizing bands with a *Tlr4* cDNA probe in the C57BL/10ScCr strain, suggesting that the absence of *Tlr4* mRNA is due to a major chromosomal rearrangement (Fig. 4 C).

Discussion

Using high-resolution genetic mapping techniques, we have restricted the position of the *Lps* gene to a 0.9-cM region of chromosome 4, flanked proximally by *D4Nds9* and distally by *D4Mit178*. A 1.7-Mb cloned DNA contig spanning this interval was sequentially assembled using YAC, BAC, and P1 clones. Our data differ significantly from another recently published physical map encompassing the *Lps* locus (37). In this contig, a gap (estimated at 100 kb by fluorescence in situ hybridization) exists in the BAC contig between *D4Nds9* and *D4Mit178*. Comparison of BAC clone addresses common to both maps suggests that this gap corresponds to the center of our contig, and is ~950 kb in size. Finally, through cDNA selection and nucleotide sequencing of randomly cloned sheared BACs from our contig, we have identified three transcription units within the *Lps* candidate region, including *Tlr4*, and two novel genes.

We provide evidence that implicates mouse *Tlr4* as a critical regulator of the innate host response to bacterial LPS. TLRs have clearly been identified as components of innate immunity against different classes of microbes in evolutionarily diverse organisms, including plants, invertebrates, and mammals (36). By using a mouse mutant that is naturally hyporesponsive to LPS, we have extended the role of TLRs, specifically *Tlr4*, to innate recognition and defense against Gram-negative bacteria in vivo. Several lines of evidence support the contention that the *Tlr4* gene is a compelling candidate for the *Lps* mutation. First, *Tlr4* maps within the genetic interval encompassing *Lps* as defined by 1,345 meioses derived from 2 independent backcrosses segregating the mutant phenotype. Second, throughout the entire *Tlr4* ORF, a single missense mutation was uniquely observed in the mutant C3H/HeJ inbred strain among all inbred strains examined, and this mutation shows exact cosegregation with the mutant *Lps* phenotype. The resulting amino acid substitution involves a highly conserved proline within the cytoplasmic signaling domain, the portion of *Tlr4* that exhibits the strongest degree of evolutionary conservation. The structural integrity of this domain appears to be essential for LPS-induced signaling by TLRs (19). The point mutation observed in the C3H/HeJ strain is not predicted to alter transcription of *Tlr4*; however, the resulting substitution of a proline residue by a basic residue would be expected to alter the topology of the *Tlr4* signaling domain and potentially disrupt protein–protein interactions with downstream molecules. Finally,

Table II. *Distribution of Nucleotide Sequence Variations in the Coding Portion of Mouse Tlr4*

	Pro^{712} (CCT)	His^{712} (CAT)
Asn^{719} (AAT)	A/J, BALB/cJ, NZW/LacJ, PERA/Ei, PERA/Rk PERC/Ei, RBA/Dn, RBB/Dn, Poschiavinos/Tirano, Poschiavinos/Zaleno, WMP/Pas, WSB/Ei	
Asn^{719} (AAC)	129/J, AKR/J, BUB/BnJ, C3H/HeN, C3H/HeOuJ, C3H/HeSnJ, C3HeB/FeJ, C57BL/6J, C57BL/10SnJ, C57BR/cdJ, C57L/J, C58/J, CE/J, DBA/2J, LP/J, NZB/BINJ, P/J, PL/J, RIIIS/J, RF/J, NOD/LtJ, SPRET/Ei, CAST/Ei, CZECH II/Ei, MOLC/Rk, MOLD/Rk, MOLE/Rk, MOLF/Ei, MOLG/Dn, *Mus caroli*, SF/CamEi, SK/CamEi, SK/CamRk, SKIVE/Ei	C3H/HeJ

corroborating evidence of a genomic deletion and absent *Tlr4* transcription was observed in C57BL/10ScCr, the other endotoxin-tolerant mouse strain known to have a mutation at the *Lps* locus. C57BL/10ScCr mice would not be expected to produce Tlr4 protein, supporting the hypothesis that their mutant phenotype results from a loss of Tlr4 function. Independent studies done by another group have also recently led to the proposal of *Tlr4* as a candidate gene for the *Lps* mutation (37).

Mammalian TLRs are part of a protein family with homologues in insects and plants, implying an ancient evolutionary origin (36). The first Toll receptor was identified during the study of embryonic development in *Drosophila melanogaster* (38). The role of this protein family in innate immune function was subsequently revealed in the adult fruit fly, as Toll mutants were unable to mount an effective antimicrobial response and succumbed to overwhelming fungal infection (39). Remarkable parallels have subsequently been identified between the Toll and IL-1R signaling pathways leading from the cell membrane to transcriptional activation within the nucleus. The cytoplasmic domains of Toll and the mammalian IL-1R (TIR domain) are homologous, and both activate signaling pathways leading to the expression of genes under the regulation of the nuclear factor (NF)-κB family of transcription factors. MyD88, an adaptor protein known to interact with IL-1R through its own TIR domain, was recently identified as a direct downstream element of the human Toll signaling pathway (36). Human Toll and IL-1R pathways share other downstream components, including the serine-threonine innate immunity kinase IRAK and TNFR-associated factor 6 (TRAF6), although the range of genes induced by these two receptors may not be identical. Additional components of these two signaling pathways are likely to be identified and will clarify their specific roles in regulation of innate immune response genes.

A family of TLRs (TLR1–5) whose genes are dispersed throughout the human genome has been identified through homology comparisons of protein architecture (17). Stable transfection of TLR2 into human embryonic kidney 293 cells induced cellular signaling, including activation of NF-κB in response to LPS and LPS binding protein (LBP), suggesting that recognition of LPS may be an attribute common to all TLRs (19). Our finding that a mutation in mouse *Tlr4* creates LPS hyporesponsiveness is consistent with and supported by these in vitro observations. An endotoxin-hyporesponsive phenotype has been documented in humans (40); however, the hypothesis that TLR4 mediates LPS-induced signaling in vivo requires further investigation. Recent observations demonstrating that the innate immune system of *Drosophila* is able to discriminate between various classes of infecting microorganisms and thereby regulate the production of different, specific antimicrobial peptides argue against significant functional redundancy of the TLR family (41).

LPS is among the most well-characterized and intensively studied bacterial virulence factors. While not intrinsically toxic, LPS is a prototypical cell stimulator capable of provoking an intense and potentially lethal host inflammatory response. A great deal is known about the intracellular events that follow LPS stimulation, yet a critical gap exists in our understanding of the mechanism by which LPS at the cell surface induces host cell activation across the cytoplasmic membrane (42, 43). In the current model, LPS monomers are catalytically transferred by a lipid exchange molecule, LBP, to CD14, a major LPS receptor that lacks a transmembrane domain (44). A putative LPS transmembrane coreceptor is then responsible for initiation of cellular responses after interaction with the LPS–CD14 complex. Based on our assertion that mutation of a transmembrane molecule creates a state of LPS hyporesponsiveness, it is conceivable that *Tlr4* is not only a strong candidate for *Lps*, but also represents a putative LPS coreceptor.

Identification of the precise mechanisms of LPS-induced cellular stimulation is of substantial significance for the understanding of bacterial pathogenesis and protective host defense. Dysregulation of the host response may lead to multiple system organ dysfunction and possible death. A molecular map of the pathways usurped by LPS will clearly be useful in future development of strategies to protect the host from the deleterious consequences of Gram-negative bacterial infection. The identification of *Tlr4* as a strong candidate for the naturally occurring mouse mutation at the *Lps* locus is reminiscent of the use of *Drosophila* mutants in the original description of Toll, and emphasizes the tremendous degree of conservation of structure and function within the innate immune system of multicellular organisms. Further studies of the role of *Tlr4* in host responses to LPS should pave the way for better understanding of the fundamental mechanisms of cellular activation.

We are grateful to Dr. Silvia Vidal and Dr. Kenneth Morgan, who made helpful suggestions during the course of this work. We thank Dr. J. Friedman for providing the *D4Rck137* probe, Dr. D. Nagle and Lisa Dirocco for assistance with BAC subcloning, Waan-Jeng Nir for help with cDNA selection, and Line Laroche for technical assistance.

This work was supported by research grants to D. Malo from the Medical Research Council of Canada and to D. Malo and P. Gros from Millennium Pharmaceuticals Inc. D. Malo is a Scholar of Fonds de la Recherche en Santé du Québec, and P. Gros is an International Research Scholar of the Howard Hughes Medical Institute and a Senior Scientist of the Medical Research Council of Canada. S.T. Qureshi is a recipient of a Clinician Scientist Award from the Medical Research Council of Canada and a Career Award in the Biomedical Sciences from the Burroughs Wellcome Fund.

Address correspondence to Danielle Malo, Centre for the Study of Host Resistance, Montreal General Hospital, 1650 Cedar Avenue, Rm. L11-144, Montreal, Quebec, H3G 1A4, Canada. Phone: 514-937-6011 ext. 4503; Fax: 514-934-8261; E-mail: mc76@musica.mcgill.ca

Received for publication 25 November 1998 and in revised form 7 December 1998.

References

1. Increases in national hospital discharge survey rates for septicemia—United States, 1979–1987. 1990. *MMWR Morb. Mortal. Wkly. Rep.* 39:31–34.
2. Glauser, M.P., D. Heumann, J.D. Baumgartner, and J. Cohen. 1994. Pathogenesis and potential strategies for prevention and treatment of septic shock: an update. *Clin. Infect. Dis.* 18:S205–S216.
3. Burrell, R. 1994. Human responses to bacterial endotoxin. *Circ. Shock.* 43:137–153.
4. Bone, R.C., R.A. Balk, F.B. Cerra, R.P. Dellinger, A.M. Fein, W.A. Knaus, R.M.H. Schein, and W.J. Sibbald. 1992. Definitions for sepsis and organ failure and guidelines for the use of innovative therapies in sepsis. *Chest.* 101:1644–1655.
5. Sultzer, B.M. 1968. Genetic control of leukocyte responses to endotoxin. *Nature.* 219:1253–1254.
6. Rosenstreich, D.L. 1985. Genetic control of the endotoxin response: C3H/HeJ mice. *In* Handbook of Endotoxin, Vol. 3. L.J. Berry, editor. Elsevier Science B.V., Amsterdam. 82–122.
7. Vogel, S.N. 1992. The *Lps* gene. Insights into the genetic and molecular basis of LPS responsiveness and macrophage differentiation. *In* Tumor Necrosis Factors: The Molecules and Their Emerging Role in Medicine. B. Beutler, editor. Raven Press, Ltd., New York. 485–513.
8. O'Brien, A.D., D.L. Rosenstreich, I. Scher, G.H. Campbell, R.P. MacDermott, and S.B. Formal. 1980. Genetic control of susceptibility to *Salmonella typhimurium* in mice: role of the *Lps* gene. *J. Immunol.* 124:20–24.
9. Glode, L.M., and D.L. Rosenstreich. 1976. Genetic control of B cell activation by bacterial lipopolysaccharide is mediated by multiple distinct genes or alleles. *J. Immunol.* 117: 2061–2066.
10. Watson, J., and R. Riblet. 1974. Genetic control of responses to bacterial lipopolysaccharides in mice. I. Evidence for a single gene that influences mitogenic and immunogenic responses to lipopolysaccharides. *J. Exp. Med.* 140:1147–1161.
11. Watson, J., R. Riblet, and B. Taylor. 1977. The response of recombinant inbred strains of mice to bacterial lipopolysaccharides. *J. Immunol.* 118:2088–2093.
12. Fultz, M.J., and S.N. Vogel. 1989. The physical separation of *Lps* and *Ifa* loci in BXH recombinant inbred mice. *J. Immunol.* 143:3001–3006.
13. Watson, J., K. Kelly, M. Largen, and B. Taylor. 1978. The genetic mapping of a defective LPS response gene in C3H/HeJ mice. *J. Immunol.* 120:422–424.
14. Vogel, S.N., J.S. Wax, P.Y. Perera, C. Padlan, M. Potter, and B.A. Mock. 1994. Construction of a BALB/c congenic mouse, C.C3H-*Lps*^{d}, that expresses the *Lps*^{d} allele: analysis of chromosome 4 markers surrounding the *Lps* gene. *Infect. Immun.* 62:4454–4459.
15. Coutinho, A., and T. Meo. 1978. Genetic basis for unresponsiveness to lipopolysaccharide in C57BL/10Cr mice. *Immunogenetics.* 7:17–24.
16. Qureshi, S.T., L. Larivière, G. Sebastiani, S. Clermont, E. Skamene, P. Gros, and D. Malo. 1996. A high-resolution map in the chromosomal region surrounding the *Lps* locus. *Genomics.* 31:283–294.
17. Rock, F.L., G. Hardiman, J.C. Timans, R.A. Kastelein, and J.F. Bazan. 1998. A family of human receptors structurally related to *Drosophila* Toll. *Proc. Natl. Acad. Sci. USA.* 95:588–593.
18. Medzhitov, R., P. Preston-Hurlburt, and C.A. Janeway, Jr. 1997. A human homologue of the *Drosophila* Toll protein signals activation of adaptive immunity. *Nature.* 388:394–397.
19. Yang, R.-B., M.R. Mark, A. Gray, A. Huang, M.H. Xie, A. Goddard, W.I. Wood, A.L. Gurney, and P.J. Godowski. 1998. Toll-like receptor-2 mediates lipopolysaccharide-induced cell signalling. *Nature.* 395:284–288.
20. Cornall, R.J., J.M. Friedman, and J.A. Todd. 1992. Mouse microsatellites from a flow-sorted 4:6 Robertsonian chromosome. *Mamm. Genome.* 3:620–624.
21. Bahary, N., D.E. McGraw, R. Shilling, and J.M. Friedman. 1993. Microdissection and microcloning of mid-chromosome 4: genetic mapping of 41 microdissection clones. *Genomics.* 16:113–122.
22. Sambrook, J., E.F. Fritsch, and T. Maniatis. 1989. Molecular Cloning: A Laboratory Manual, 2nd ed. Cold Spring Harbor Laboratory, Cold Spring Harbor, NY.
23. Feinberg, A.P., and B. Vogelstein. 1983. A technique for radiolabeling DNA restriction endonuclease fragments to high specific activity. *Anal. Biochem.* 132:6–13.
24. Kusumi, K., J.S. Smith, J.A. Segre, D.S. Koos, and E.S. Lander. 1993. Construction of a large-insert yeast artificial chromosome library of the mouse. *Mamm. Genome.* 4:391–392.
25. Shizuya, H., B. Birren, U.J. Kim, V. Mancino, T. Slepak, Y. Tachliri, and M. Simon. 1992. Cloning and stable maintenance of 300-kilobase-pair fragments of human DNA in *Escherichia coli* using an F-factor-based vector. *Proc. Natl. Acad. Sci. USA.* 89:8794–8797.
26. Dracopoli, N.C., J.L. Haines, B.R. Korf, D.T. Moir, C.C. Morton, C.E. Seidman, J.G. Seidman, and D.R. Smith. 1994–1997. Current Protocols in Human Genetics, Vol. 1. John Wiley & Sons, Inc., New York.
27. Malo, D., S. Vidal, J.H. Lieman, D.C. Ward, and P. Gros. 1993. Physical delineation of the minimal chromosomal segment encompassing the murine host resistance locus *Bcg*. *Genomics.* 17:667–675.
28. Carle, G.F., and M.V. Olson. 1984. Separation of chromosomal DNA molecules from yeast by orthogonal-field-alteration gel electrophoresis. *Nucleic Acids Res.* 12:5647–5664.
29. Vidal, S.M., D. Malo, K. Vogan, E. Skamene, and P. Gros. 1993. Natural resistance to infection with intracellular parasite: isolation of a candidate for *Bcg*. *Cell.* 73:469–485.
30. Rommens, J.M., L. Mar, J. McArthur, L.-C. Tsui, and S.W. Scherer. 1994. Towards a transcriptional map of the q21-q22 region of chromosome 7. *In* Identification of Transcribed Sequences. U. Hochgeschwender and K. Gardiner, editors. Plenum Press, New York. 65–79.

31. Lennon, G., C. Auffray, M. Polymeropoulos, and M.B. Soares. 1996. The I.M.A.G.E. Consortium: an integrated molecular analysis of genomes and their expression. *Genomics*. 33:151–152.
32. Silahtaroglu, A.N., Z. Tumer, T. Kristensen, L. Sottrup-Jensen, and N. Tommerup. 1993. Assignment of the human gene for pregnancy-associated plasma protein A (*PAPPA*) to 9q33.1 by fluorescence in situ hybridization to mitotic and meiotic chromosomes. *Cytogenet. Cell Genet*. 62:214–216.
33. Fridell, R.A., L.S. Harding, H.P. Bogerd, and B.R. Cullen. 1995. Identification of a novel human zinc finger protein that specifically interacts with the activation domain of lentiviral Tat proteins. *Virology*. 209:347–357.
34. Zheng, C., N. Heintz, and M. Hatten. 1996. CNS gene encoding astrotactin, which supports neuronal migration along glial fibres. *Science*. 272:417–419.
35. Kobe, B., and J. Deisenhofer. Crystal structure of porcine ribonuclease inhibitor, a protein with leucine-rich repeats. 1993. *Nature*. 366:751–756.
36. Medzhitov, R., P. Preston-Hurlburt, E. Kopp, A. Stadien, C. Chen, S. Ghosh, and C.A. Janeway, Jr. 1998. MyD88 is an adaptor protein in the hToll/IL-1 receptor family signaling pathways. *Mol. Cell*. 2:253–258.
37. Poltorak, A., I. Smirnova, X. He, M.-Y. Liu, C. Van Huffel, D. Birdwell, E. Alejos, M. Silva, X. Du, P. Thompson, et al. 1998. Genetic and physical mapping of the *lps* locus: identification of toll-4 receptor as a candidate gene in the critical region. *Blood Cells Mol. Dis*. 15:340–355.
38. Hashimoto, D., K.L. Hudson, and K.V. Anderson. 1988. The *Toll* gene of *Drosophila*, required for dorso-ventral embryonic polarity, appears to encode a transmembrane protein. *Cell*. 52:269–279.
39. Lemaitre, B., E. Nicolas, L. Michaut, J.-M. Reichhart, and J. Hoffman. 1996. The dorsoventral regulatory gene cassette *spätzle/Toll/cactus* controls the potent antifungal response in *Drosophila* adults. *Cell*. 86:973–983.
40. Kuhns, D.B., D.A. Long Priel, and J.I. Gallin. 1997. Endotoxin and IL-1 hyporesponsiveness in a patient with recurrent bacterial infections. *J. Immunol*. 158:3959–3964.
41. Lemaitre, B., J.-M. Reichhart, and J. Hoffman. 1997. *Drosophila* host defense: differential induction of antimicrobial peptides after infection by various classes of microorganisms. *Proc. Natl. Acad. Sci. USA*. 94:14614–14619.
42. Raetz, C.R.H., R.J. Ulevitch, S.D. Wright, C.H. Sibley, A. Ding, and C.F. Nathan. 1991. Gram-negative endotoxin: an extraordinary lipid with profound effects on eukaryotic signal transduction. *FASEB J.* 5:2652–2660.
43. Ulevitch, R.J., and P.S. Tobias. 1995. Receptor-dependent mechanisms of cell stimulation by bacterial endotoxin. *Annu. Rev. Immunol*. 13:437–457.
44. Yu, B., and S.D. Wright. 1996. Catalytic properties of lipopolysaccharide (LPS) binding protein. *J. Biol. Chem*. 271: 4100–4105.

Qureshi et al. Vol. 189, No. 4, February 15, 1999. Pages 615–625.

The authors regret that two references that apply directly to the data they presented were not cited. The details of these omissions follow.

During the course of the above work, the positional cloning of *Lps* was reported (Poltorak, A., X. He, I. Smirnova, M.Y. Liu, C.V. Huffel, X. Du, D. Birdwell, E. Alejos, M. Silva, C. Galanos, M. Freudenberg, P. Ricciardi-Castagnoli, B. Layton, and B. Beutler. 1998. *Science*. 282:2085–2088). A preliminary report of these findings had been presented at the 12th International Mouse Genome Conference in Germany, September 28–October 3, 1998.

The RNA and DNA samples used to generate Fig. 4 were derived from the LPS-hyporesponsive C57BL/10ScNCr strain (National Cancer Institute, Frederick, MD), the progenitor for C57BL/10ScCr (Vogel, S.N., C.T. Hansen, and D.L. Rosenstreich. 1979. *J. Immunol*. 122:619–622). Reference to C57BL/10ScCr in the text should read as C57BL/10ScNCr.